Published in final edited form as:
Int Rev Neurobiol. 2009 ; 88: 65–100. doi:10.1016/S0074-7742(09)88004-5.

Acute Methamphetamine Intoxication: Brain Hyperthermia, Blood-Brain Barrier and Brain Edema

Eugene A. Kiyatkin[a,*] and **Hari S. Sharma**[a,b]

[a]Behavioral Neuroscience Branch, National Institute on Drug Abuse–Intramural Research Program, National Institutes of Health, 333 Cassell Drive, Baltimore, MD 21224, USA

[b]Laboratory of Cerebrovascular Research, Department of Surgical Sciences, University Hospital, Uppsala University, Frödingsgatan 12, #28, SE-751 85 Uppsala, Sweden

Abstract

Methamphetamine (METH) is a powerful and often abused stimulant with potent addictive and neurotoxic properties. While it is generally assumed that multiple chemical substances released in the brain following METH-induced metabolic activation (or oxidative stress) are primary factors underlying damage of neural cells, in this work we will present data suggesting a role of brain hyperthermia and associated leakage of the brain-blood barrier (BBB) in acute METH-induced toxicity. First, we show that METH induces a dose-dependent brain and body hyperthermia, which is strongly potentiated by associated physiological activation and in warm environments that prevent proper heat dissipation to the external environment. Second, we demonstrate that acute METH intoxication induces robust, widespread but structure-specific leakage of the BBB, acute glial activation, and increased water content (edema), which are related to drug-induced brain hyperthermia. Third, we document widespread morphological abnormalities of brain cells, including neurons, glia, epithelial and endothelial cells developing rapidly during acute METH intoxication. These structural abnormalities are tightly related to the extent of brain hyperthermia, leakage of the BBB, and brain edema. While it is unclear whether these rapidly developed morphological abnormalities are reversible, this study demonstrates that METH induces multiple functional and structural perturbations in the brain, determining its acute toxicity and possibly contributing to neurotoxicity.

I. Introduction

Methamphetamine (METH) is a powerful and often abused psychomotor stimulant with potent addictive and neurotoxic properties. In addition to the social harms of addiction, the use of this substance could adversely influence human health, causing acute behavioral and physiological disturbances during intoxication and long-term health complications following chronic use (Kalant, 2001). METH abuse could also be a cofactor enhancing different latent pathological conditions, especially cardiovascular, neurological and psychiatric, as well as increasing the probability and severity of numerous viral and bacterial infections.

Considering the issue of neurotoxicity, it is usually assumed that METH has direct toxic effects on neural cells, with relative selectivity towards specific cell groups, brain structures, and cellular organelles. In particular, METH preferentially affects midbrain dopamine (DA) cells, damaging fine axonal terminals in the striatum (Ricaurte et al., 1980; Riddle et al., 2006; Woolverton et al., 1989) and resulting in health complications associated with

Corresponding Author: Eugene A. Kiyatkin, MD, PhD; Behavioral Neuroscience Branch, NIDA–IRP, NIH, 333 Cassell Drive, Baltimore, MD 21224, USA; tel.: 443-740-2844; fax: 443-740-2155; ekiyatki@intra.nida.nih.gov.

pathologically altered DA transmission. Particularly, perturbations in DA as well as other monoamine systems are an important factor in psycho-emotional and movement disorders including acute METH psychosis and severe depression following long-term METH use and withdrawal (Kalant, 2001).

However, METH also induces metabolic activation (Estler, 1975; Makisumi et al., 1998) and hyperthermia (Alberts and Sonsalla, 1995; Kalant and Kalant, 1975; Sandoval et al., 2000). Enhanced metabolism is tightly related to oxidative stress, which is caused by an imbalance between the production of reactive oxygen and a biological system's ability to detoxify readily the reactive intermediates or easily repair the resulting damage. Disturbances in this normal redox state can cause toxic effects through the production of peroxides and free radicals that damage all components of the cell, including proteins, lipids, and DNA. Oxidative stress as a consequence of brain hyper-metabolism is usually viewed as a primary factor in METH-induced neurotoxicity (Cadet et al., 2007; De Vito and Wagner, 1989; Stephans and Yamamoto, 1994; Yamamoto and Zhu, 1998). On the other hand, brain cells are exceptionally temperature-sensitive, with the appearance of irreversible changes in structure and functions at ~40°C, i.e., only three degrees above normal baseline (Iwagami, 1996; Chen et al., 2003; Oifa and Kleshchenov, 1985; Sharma and Hoopes, 2003). Due to the strong temperature-dependence of most physico-chemical processes governing neural activity (see Kiyatkin, 2005 for review), hyperthermia could also strongly modulate toxic effects of METH on brain cells. It is well known that METH is much more toxic at high environmental temperatures, while toxicity is diminished by low ambient temperatures (Alberts and Sonsalla, 1995; Ali et al., 1994; Bowyer et al., 1993; Farfel et al., 1995; Miller and O'Callaghan, 1994). While it is reasonable to assume that the more harmful effects of METH seen in warm, humid conditions are associated with intra-brain heat accumulation due to enhanced brain metabolism coupled with the diminished ability to dissipate properly metabolic heat, direct data on brain temperature changes induced by METH and its environmental modulation are limited.

In addition to the direct effects of high temperatures on brain cells and potentiation of toxic effects of brain metabolites, brain hyperthermia appears to affect the permeability of the blood-brain barrier (BBB). The BBB is an important border that protects the brain environment, while BBB leakage allows water, ions, and various potentially neurotoxic substances contained in blood plasma (i.e., glutamate) to enter the brain (Rapoport, 1976; Zlokovic, 2008). Although leakage of the BBB has been documented during environmental warming (Sharma et al., 1992; Cervos-Navarro et al., 1998), intense physical exercise (Watson et al., 2006), various types of stress (Esposito et al., 2001; Ovadia et al., 2001; Sharma and Dey, 1986) and morphine withdrawal (Sharma and Ali, 2006), data on METH-induced alterations in the BBB and its relationship to brain temperature are limited.

In this work we present and discuss several sets of recent data, suggesting a tight link between acute METH toxicity, brain temperature, and alterations of the BBB. Based on published literature and these data we demonstrate that brain hyperthermia induced by METH plays an important role in the triggering of several pathophysiological mechanisms underlying acute toxicity of this drug and contributing to neurotoxicity.

II. Basic terminology and major topics of this study

Drug toxicity is generally defined as a degree to which a chemical toxin is able to damage an exposed organism. Toxicity can refer to the effect on a whole organism as well as the effect on a substructure such as a cell (citotoxicity), an organ (organotoxicity), or specific tissue. Therefore, *neurotoxicity* usually refers to adverse effects on the structure or function of the central and/or peripheral nervous system. Clinically, neurotoxicity is measured based on

specific symptoms (i.e. muscle weakness, loss of sensation and motor control, tremors, cognitive alterations, or autonomic nervous system dysfunctions), but in the experimental work, it is typically defined as neural damage, the analysis of which requires post-mortem examination of brain tissue. The term 'neural damage', moreover, is not precise because it could mean morphological or functional abnormalities of specific brain cells or cell groups, which contrast to a certain morphological and functional 'norm' and could suggest that these cells will degenerate in the future. This approach allows one to detect early changes that could finally result in cellular death, but it fails to differentiate clearly between reversible and irreversible damage. On the other hand, neural damage could be verified by detection of dead cells, but significant time is always necessary for a normal cell to become damaged, for the damage to become irreversible, and for an irreversibly damaged cell to die and be recognized as dead. Moreover, dead cells are effectively eliminated from brain tissue by phagocytosis and their detection in brain tissue has a relatively short window of time (see Bowyer and Ali, 2006). Irreversible structural abnormalities could be better verified with the use of electronic microscopy but the use of this technique for the study of METH neurotoxicity is limited.

Another important issue of toxicity is the drug's dose-dependence. The effects are absent or undetectable at low doses, they progress at larger doses, and finally result in lethality at high doses. Toxicity could be measured by the drug's effects on a particular target (organism, organ, tissue, or cell) and at the level of the whole organism it could be quantified based on LD50. The LD50 for METH with intraperitoneal (ip) administration is 55 and 57 mg/kg, in rat and mouse, respectively (Davis et al., 1987; Yamamoto, 1963). While an important measure to grade a degree of toxicity, LD50 could be misleading because the toxic effects of METH in humans differ from those in experimental animals, are strongly modulated by environmental conditions, depend on age and activity state, and are influenced by co-use of other substances and individual sensitivity. For example, ~80% of rats that received 9 mg/kg of METH (i.e., 1/6 of a traditional LD50) died within 6 hours when the injection was done at 29°C ambient temperature (Brown and Kiyatkin, 2005). This temperature is only 5–6°C above the laboratory standard, corresponding to normothermia or temperature comfort (Romanovsky et al., 2002) and has no evident effects on basal temperature and animal behavior (Kiyatkin and Brown, 2004). Therefore, under specific conditions, the drug could be toxic at the doses incomparably lower than traditional LD50 values. This feature could be especially important for psychomotor stimulant drugs, which are often taken under specific activity states and environmental conditions such as raves, when individuals are highly active, exposed to warm and humid conditions, and their ability to dissipate heat is limited.

Brain temperature and brain thermal homeostasis are other important topics of this work. *Hyperthermia* (or *hypothermia*) in this study defines an increase (or decrease) in temperature. Depending upon location, hyperthermia (or hypothermia) could occur in the brain, muscles, body core, and skin. Traditionally, hyperthermia is contrasted to fever (pyrexia), an increase in internal temperature, which occurs due to temporary elevation of the body's thermoregulatory set-point, a conceptual mechanism that was proposed to explain body temperature regulation (see Romanovsky, 2003 for discussion). Fever is usually viewed as an organism's induced temperature increase, when heat is produced and actively retained in the body by decreased heat dissipation. In contrast, hyperthermia defines body temperature increase that occurs without the consent of the heat control system, i.e. over the body thermoregulatory set-point; in this case, the body produces (or absorbs from outside) more heat than it can dissipate. While the discussion of these issues is clearly out of the scope of the present work, brain temperature alterations induced by psychomotor stimulant drugs are determined by their specific actions on neural substrates, affecting brain and body metabolism and inducing behavioral and physiological effects (see Kiyatkin, 2005, 2006 for further review). These drugs also have vasoconstrictive effects, limiting heat dissipation to

the external environment and potentiating brain and body hyperthermia. Therefore, as we will show below, hyperthermia induced by METH and other related drugs mimic some important aspects of fever, i.e. active temperature increase.

METH-induced change in the permeability of the *blood-brain barrier* (BBB) is another important topic of this work. The BBB is a highly specialized brain-endothelial structure of the fully differentiated neurovascular system. In concert with pericytes, astrocytes, and microglia, the BBB separates components of the circulating blood from neurons and maintains the chemical composition of the intra-brain environment, which is required for proper functioning of neural circuits, synaptic transmission, synaptic remodeling, angiogenesis, and neurogenesis. BBB breakdown, due to disruption of the tight junctions and altered transport of molecules between the blood and brain, may initiate various pathophysiological mechanisms resulting in robust brain abnormalities and serious health complications (see Zlokovic, 2008 for review). While alterations in the permeability of the BBB are implicated in the development and progression of various neurodegenerative disorders (Alzheimer's disease, Parkinson's disease, amyotrophic lateral sclerosis, multiple sclerosis), we will demonstrate that METH also seriously alters BBB permeability, triggering a link of pathophysiological processes that contribute to both acute drug toxicity and neurotoxicity.

III. Brain temperature responses to METH are dose-dependent and modulated by activity state and environmental conditions

The effects of addictive drugs are usually studied in animals under well-controlled experimental conditions. In addition to standard temperature and humidity, drugs are typically administered after animals' habituation to the testing environment and under quiet resting conditions when baselines are stable and low. In contrast, humans often use the same drugs voluntarily, in different doses, under conditions of psychophysiological activation (that usually precedes drug intake) and in specific environmental conditions that often dramatically differ from those in animal experiments. For example, METH and other psychomotor stimulant drugs (i.e., MDMA) are often taken during raves, when the drug intake is associated with a high degree of psychophysiological and behavioral activation and adverse environmental conditions (hot and humid environment) that seriously impact an organism's thermoregulatory mechanisms. To examine how the effects of psychomotor stimulants are modulated by activity states and environmental conditions, we performed a series of studies, focusing on brain temperature as a primary parameter of interest (Brown et al., 2003; Brown and Kiyatkin, 2004, 2005). First, we examined how METH, at different doses, affects brain temperature and what the relationships between these temperatures and those recorded from various body locations are. Second, we examined how thermal effects of this drug are modulated during associated physiological activation and in a moderately hot environment. To model psychophysiological activation, we used the procedure of social interaction, in which the recorded male rat was exposed to a female rat, resulting in behavioral activation and a clear temperature response. The effects of METH were also compared in two ambient temperatures: 23°C and 29°C. Finally, to clarify the mechanisms underlying brain hyperthermic effects of psychomotor stimulants, we examined how these effects are modulated by functionally diminished blood outflow from the brain. To model this condition, both jugular veins, which provide >90% of blood outflow from the brain (Doepp et al., 2004), were sequentially surgically closed. Animals with blocked jugular veins were seemingly normal, gained weight, showed generally normal responses to environmental challenges and had basal brain or body temperature similar to those in control rats.

Our studies revealed that METH induces dose-dependent temperature increases, which were generally correlative in different brain sites (NAcc, hippocampus), temporal muscle, and body core. At the lowest dose (1 mg/kg, sc), the increase had the smallest amplitude and duration (~1.0°C for ~160 min) and was progressively larger and more prolonged at moderate (3 mg/kg; 1.4°C for 280 min) and high (9 mg/kg: ~3.4°C for 360 min) doses. At the latter dose (see Fig. 1A), brain hyperthermia even in standard ambient temperatures (22–23°C), reached clearly pathological levels (~40°C or 3.5°C above baseline). This temperature increase generally correlated with locomotor hyperactivity, which was evident and strong at 1 mg/kg and greatly progressed (with the addition of strong stereotypy) at higher doses. Although drug-induced temperature changes were generally correlative in brain structures, muscle, and body core, each point has its own temperature. Within the brain, temperatures are distributed according to a dorso-ventral gradient (cortex<hippocampus< thalamus, dorsal striatum<ventral striatum, hypothalamus) and for ventrally located structures (i.e., NAcc), they are ~1°C higher than in temporal muscle and about the same as in the body core. Skin has the lowest temperature, about 1°C less than in the muscle and ~2°C less than in ventral brain structures (ventral striatum, hypothalamus).

The hyperthermic response to METH had two important features (see Fig. 1, left panel). First, although temperatures in the NAcc and hippocampus generally paralleled those in temporal muscle (Fig. 1A), the increases were significantly more rapid and stronger in the brain than temporal muscle, resulting in significant increases in brain-muscle differentials (Fig. 1C). Therefore, it appears that metabolic brain activation associated with intra-brain heat production is the primary cause of brain hyperthermia and a factor behind more delayed and weaker body hyperthermia. At a 9 mg/kg METH dose, the increase in the NAcc-muscle differential was robust and continued for more than five hours, suggesting a pathological aspect to this brain hyperthermia. Second, temperature increase in brain sites and muscle was consistently associated with a rapid, transient decrease in skin temperature, suggesting acute vasoconstriction. Therefore, decreased heat dissipation to the external environment is another important factor contributing to overall brain and body hyperthermia.

Hyperthermic effects of METH became stronger when the drug was injected during social interaction. As shown in Fig. 1 (middle panel), after presentation of the female, the recorded male showed a strong increase in brain and body temperatures. When METH was injected under these conditions, drug-induced temperature increase became stronger in both brain areas. While the effect was not additive, METH-induced brain hyperthermia during social interaction reached significantly higher values and was maintained for a significantly longer time than in quiet resting conditions.

Hyperthermic effects of METH were also altered when the drug was administered in a warm environment. As shown in Fig. 1 (right panel), mean temperatures after drug administration increased rapidly in all animals, in some of them the increase reached clearly pathological values (>41 °C), and 4/6 animals died within three hours. One more animal, which showed a strong and stable hyperthermia (~40.6 °C) died overnight. Importantly, temperature increases in the brain sites were consistently more rapid and stronger and the increase in NAcc-muscle differential reached pathological levels not seen in any other physiological conditions (see Fig. 1B). However, at the moment of death, brain-muscle differentials rapidly inverted and the brain became cooler than the body (Fig. 1C).

Similar data were also obtained with MDMA, another widely used psychomotor stimulant drug (Brown and Kiyatkin, 2004). Although MDMA induced weaker increases in brain and body temperatures at similar doses (and even induced mild hypothermia at 1 mg/kg dose), these effects were strongly potentiated during social interaction (+89%) and in a warm environment (29°C; +268%). Similar to METH, three of six tested animals that showed

maximal temperature increases (>41 °C) after MDMA at 9 mg/kg died within four hours and two more rats died at the fifth post-drug hour. Similar to METH, rats also showed dramatic increases in brain-muscle differentials, which peaked close to the moment of death but inverted rapidly when the rat stopped breathing and the brain became relatively cooler than the body. In the case of MDMA, we also evaluated how diminished blood outflow affects drug-induced hyperthermic responses. Compared to control animals, the hyperthermic response to MDMA in rats with blockade of both jugular veins was strongly potentiated (+188%), with a much greater increase in brain-muscle temperature differentials. Therefore, MDMA-induced brain hyperthermia results from intra-brain heat production, while venous outflow is an important means for heat dissipation from the brain to the rest of the body.

Classic features of neurotoxicity induced by amphetamine-like substances (i.e., neuronal necrosis and apoptosis) are usually linked to some toxic products (i.e., nitric oxide, catechol-quinones, peroxynitrite) of abnormally increased metabolism of endogenous neurotransmitter substances (Cadet et al., 2001; Kuhn and Geddes, 2000). While these factors may contribute to neural damage following chronic use of these substances, our present data suggest the importance of brain overheating as a factor responsible for fatal decompensation of an organism's vital functions due to an acute drug intoxication. The rise in brain temperature above certain 'normal' limits may *per se* have a directly destructive action on brain cells, which will increase exponentially with slight increases above these limits. The most temperature-sensitive cellular elements are mitochondrial and cellular membranes, in which irreversible transitions in protein structure or arrangements begin to occur at temperatures higher than 40 °C (Iwagami et al., 1996; Lepock, 2003; Willis et al., 2000). Therefore, 40 °C could be considered the threshold of pathological hyperthermia, which could have long-term negative consequences even if the temperature will later return to its baselines.

Since the rats that died following METH and MDMA intoxication in a moderately warm environment showed some clinical features suggesting brain edema, we hypothesized that the destruction of endothelial cells in the brain and leakage of serum proteins across the BBB induced by high temperature could be an important pathogenic factor responsible for this life-threatening condition. The next chapter will present the results of our recent experiments aimed at verification of this hypothesis (Kiyatkin et al., 2007; Sharma and Kiyatkin, 2009).

IV. Acute METH intoxication results in BBB leakage, acute glial activation and morphological alterations of brain cells: role of brain temperature

Similar to our previous thermorecording experiments, rats were implanted with three thermocouple electrodes (NAcc, temporal muscle, and skin) and an intravenous (iv) jugular catheter, habituated to the experimental conditions, and divided in three groups. Rats from the first two groups received METH (9 mg/kg, sc) in normal (23°C) and warm (29°C) conditions, respectively. When brain temperature peaked or reached clearly pathological values (>41.5°C), the rats were injected with Evans blue (EB), rapidly iv anesthetized with pentobarbital, perfused, and brains were taken for analysis. Control animals received saline and underwent the same procedures as METH-treated rats. The state of BBB permeability and edema were determined by diffusion into brain tissue of Evans Blue dye, an exogenous tracer that is normally retained by the BBB, and measuring brain water and ion (Na^+, K^+, Cl^-) content. Immunohistochemistry was used to evaluate quantitatively brain presence of albumin, a measure of breakdown of the BBB, and glial fibrillary acidic protein (GFAP), an index of astrocytic activation. Albumin is a relatively large plasma protein (molecular weight 59 kDa, molecular diameter 70A) that is normally confined to the luminal side of the endothelial cells and is not present in the brain. Similarly, EB, the exogenous protein tracer

that binds to plasma albumin, fails to enter the brain from the peripheral circulation (Blezer, 2005; Ehrlich, 1904; Sharma, 2007). Thus, the presence of EB in the brain, the appearance of albumin-positive cells, and albumin immunoreactivity in the neuropil indicate a breakdown of the BBB. GFAP is an intermediate filament protein that is expressed in glial cells (astrocytes). Increased GFAP immunoreactivity (or astrocytic activation) is usually viewed as an index of gliosis or a relatively slow-developing correlate of neural damage (Finch, 2003; Hausmann, 2003). Normal brain tissue has only scattered GFAP-positive cells but rapid GFAP expression has been reported previously during environmental warming and brain trauma (Cervos-Nacarro et al., 1998; Gordth et al., 2006).

To determine morphological abnormalities of brain cells, slices were stained with haemotoxylin-eosin or Nissl and analyzed with light microscopy to determine the extent and specifics of structurally abnormal cells. Brain slices were also immunostained for myelin basic protein (MBP) and stained for luxol fast blue to identify myelinated and unmyelinated nerve fibers and study changes in myelin function. For more detailed analyses of cellular and subcellular alterations, we also used transmission electronic microscopy (TEM). To determine the specificity of METH-induced changes in brain parameters, they were determined separately in the cortex, hippocampus, thalamus, and hypothalamus.

1. Alterations in the BBB permeability

As shown in Fig. 2, METH induced significant and widespread BBB leakage. Compared to saline-treated controls, both EB (A) and albumin immunoreactivity (B) increased strongly in both METH groups and the changes were significantly larger when the drug was administered at 29° than 23°C. At the time when brains were taken, these two subgroups of animals had significantly higher NAcc (23°C: 38.92±0.34°C and 29°C: 41.37±0.22°C) and muscle temperatures (23°C: 37.92±0.32°C and 29°C: 40.44±0.19°C) compared to controls (36.67±0.14°C and 35.82±0.08°C in the NAcc and muscle, respectively). Moreover, the amplitude of temperature response in both locations was significantly stronger at 29°C than 23°C. While the changes in EB occurred in each brain structure, there were some between-structural differences. The cortex showed minimal EB content, followed by the hippocampus, thalamus, and hypothalamus, which all had a higher EB content than cortical tissue. However, the increase with METH-23°C was stronger in the cortex (+133 %) and hippocampus (+134 %) and weaker in hypothalamus (+71%) and thalamus (+66 %). Similar differences were seen with METH-29°C; the increase was greatest in the cortex (+390%), followed by hippocampus (+261 %), hypothalamus (+109 %), and thalamus (+107 %).

Albumin immunoreactivity showed similar but stronger changes. As shown in a representative example of immunostained cortical tissue (see Fig. 3a, d, g), the leakage of albumin in the neuropil was evident in animals that received METH and was more prominent in animals that were exposed to the drug at 29°C (g) than 23°C (d). Quantitative analysis of albumin-positive cells (Fig. 2B) showed a significant increase in each brain structure, which was again maximal in the cortex and hippocampus and lower in the thalamus and hypothalamus. The number of albumin-positive cells was significantly higher when METH was administered at 29°C than 23°C. Again, the cerebral cortex and hippocampus showed the strongest increase (29.25±1.60 immunopositive cells/section or 49-fold vs. control and 26.88±1.13 immunopositive cells/section or 24-fold vs. control), followed by the thalamus (17.88±1.13), and hypothalamus (15.00±0.78).

As shown in Fig. 2C, there was a strong liner correlation between concentrations of EB and numbers of albumin-positive cells (r=0.90 for the cortex), suggesting tight relationships between these two measures of BBB permeability. Albumin immunoreactivity was also strongly dependent on brain temperature (r=0.91 for the cortex), with virtually no positive cells at low basal temperatures and a progressive increase at high temperatures (Fig. 2D).

This correlation was evident in each brain structure and equally strong with respect to brain and muscle hyperthermia.

2. Glial changes

As shown in Fig.4, only a few GFAP-positive astrocytes were scattered in the normal brains; the hippocampus showed more stained cells than thalamus, cortex, and hypothalamus. In the METH-23°C group, the number of GFAP-positive cells was significantly larger, with the greatest increase in the thalamus followed by the hippocampus, cortex, and hypothalamus (A). In the METH-29vC group, the number of GFAP-positive astrocytes was almost doubled in the cortex and hippocampus and 1.5 times higher in the hypothalamus and thalamus compared to the METH-23°C group. A representative example of GFAP-positive cells during METH treatment is shown in Fig. 3 (c, f, i). While a few GFAP-positive cells (arrowhead) are seen in the control thalamus (c), their numbers were larger in the METH-23°C (f) and especially in the METH-29°C group (i). In the backgrounds, damaged nerve cells and perineuronal edema were often seen around areas of GFAP expression in these animals.

Changes in GFAP immunoreactivity were tightly and linearly correlated with albumin immunoreactivity (Fig. 4B), suggesting close relationships between leakage of the BBB and acute glial reaction. GFAP counts were also tightly correlated with brain temperatures (Fig. 4C), suggesting that acute glial reaction is progressively larger depending on the extent of brain temperature elevation.

3. Alterations in water and ion content

In agreement with the previous findings on regional differences in brain water content (Rapoport, 1976), we found that the hippocampus has a higher water content (78.4%) than the cortex (74.5%) and the underlying thalamus (75.5%) and hypothalamus (75.5%) in control conditions (Fig. 5A). METH administered at 23°C induced a significant and strong increase in water content in each structure, but as a relative change, the increase was similar in the cortex, hippocampus and thalamus (1.3–1.4%) but weaker in the hypothalamus (0.9%). The increase was dramatically larger in the METH-29°C group but the pattern did not differ significantly in various structures. Thus, the cortex and hypothalamus exhibited about 2.9 and 3.1% increases, respectively, over control values, while the thalamus and hypothalamus showed 2.8 and 2.6% elevations. In each brain structure, tissue water content was directly related to albumin immunoreactivity (B) and brain temperatures (C), suggesting tight relationships between brain temperature, changes in BBB permeability, and edema.

METH treatment also resulted in a general increase in Na^+, K^+ and Cl^- contents in various brain areas; this increase was stronger when METH was used at 29°C than 23°C (Fig. 6A–C). The regional contents of each ion varied, with the highest absolute levels for Na^+, lower for K^+, and lowest for Cl^-. Na^+, K^+ and Cl^- contents in control were highest in the hippocampus, followed by the cortex, and lowest in the hypothalamus and thalamus. With respect to Na^+, the increase seen in the METH-23°C group vs. control was significant and almost identical in each structure (+30–36 mM/kg). With respect to K^+ and Cl^-, the increase was structure-selective, with no changes of K^+ in the cortex and hippocampus and no changes in Cl^- in hippocampus and hypothalamus in the METH-23°C group. In fact, K^+ levels in the cortex were even lower than in control. However, the levels of all ions were significantly higher in the METH-29°C vs. control groups. With respect to Na^+, the increase was the most pronounced, with maximal change in hypothalamus (+72 mM/kg) and thalamus (+62 mM/kg). These two structures also showed maximal increases in Cl− (32 nM and 33 nM, respectively), although the increases in this ion were qualitatively lower than

those for Na^+. The increases in K^+ were maximal in the thalamus (+67 mM), followed by the hippocampus and hypothalamus (44 and 42 mM), and minimal in the cortex (29 mM).

Although concentrations of each ion significantly correlated with both water content (Fig. 6E) and brain temperatures (E), the correlation was strongest for Na^+, weaker for Cl^-, and minimal for K^+.

4. Morphological changes

4.1. Neuronal Changes—As shown in Fig. 7, METH treatment resulted in a profound increase in the amount of abnormal neural cells in each studied brain structure. The increase was significant in each region but the highest numbers were seen in the hippocampus followed by the thalamus, hypothalamus, and cortex. In terms of relative change, the hippocampus also showed the maximal effect (×52), followed by hypothalamus (×30), cortex (×21), and thalamus (×20). The incidence of neuronal damage was almost 1.5 times greater in animals that received METH at 29°C. In this case, the greatest changes were seen in the cortex, followed by the hippocampus, thalamus, and hypothalamus.

Representative examples of Nissl-stained sections showing nerve cell damage in the cerebral cortex are depicted in Fig. 8. Normal animals exhibit healthy neurons with a distinct nucleus and clear cytoplasm (a). Occasionally, a few neurons show a dense cytoplasm with a slightly excentric nucleus (arrow head). On the other hand, several pyknotic neurons (c and e, arrows), perineuronal edema, sponginess, and expansion of the cortex were seen in METH-treated rats.

4.2. Damage to choroid epithelial cells—METH also induced marked damage to the choroid plexus, a substrate of the blood-cerebrospinal fluid (CSF) barrier. While choroid epithelium in control brains consists of compact and dense epithelial cells with a distinct nucleus (Fig. 8b; arrow-heads), marked degeneration of epithelial cells with occasional staining of cell nuclei was found in METH-23°C rats (d). These changes were most prominent in the METH-29°C group, where massive degeneration of epithelia with no distinction between individual cell nuclei and epithelial cells was apparent (f).

4.3. Myelin Changes—Since damage of myelin is quite common following BBB breakdown in various experimental and clinical conditions (see Sharma and Westman, 2004 for review), we examined myelin damage in METH-treated rats using myelin basic protein (MBP) immunoreactivity (see Figs. 3b, e, h). In normal animals, myelinated fibers and bundles are very dense red with MBP immunostaining (b), corresponding to intact myelin sheaths and myelinated axons. In contrast, degradation of MBP (e and h) seen in METH-treated animals reflects markedly degenerated myelinated fibers and axons; this decrease in myelin was greater when METH was administered to rats at 29° C (h). Degeneration of myelin was commonly seen in the areas showing edematous expansion of the neuropil (h).

4.4. Relationships between brain damage and other parameters—Changes in brain morphology were associated with profound changes in all other analyzed parameters (Fig. 7). As can be seen in Fig. 7B, cortical neural damage during METH intoxication was tightly related to *albumin leakage* (r=0.93, 0.90, 0.89 and 0.90 for the cortex, hippocampus, thalamus, and hypothalamus, respectively). In the control cortex, when albumin leakage was virtually absent, there were no abnormal cells but their number grew progressively in METH-treated brains, depending on the extent of brain hyperthermia. The number of abnormal cells also tightly correlated with extent of *GFAP immunostaining* (Fig. 7B). This correlation was strong, linear, and virtually equal in all other structures (r=0.88, 0.90, 0.90

and 0.90 for the cortex, hippocampus, thalamus, and hypothalamus, respectively), indicating its generality for the brain as a whole.

The number of damaged cortical cells during METH intoxication correlates linearly with *water accumulation* in all brain areas (see Fig. 7C for the cortex). This relationship appears to be a reflection of generalized edema, which progresses when METH is used at 29°C, resulting in more profound cellular damage. Finally, structural damage was tightly related to *brain temperature* (Fig. 7D). While damaged cell count increased proportionally with temperature, the intensity of damage in each structure was independent of absolute temperatures. While brain temperature was recorded only from the NAcc in this study, it should follow a dorso-ventral temperature gradient and be minimal in the cortex, lower in hippocampus and thalamus, and maximal in the hypothalamus (see Kiyatkin, 2005). However, the damage in 'warm' hypothalamus during METH intoxication was minimal but was maximal in the 'cool' cortex.

More important, METH-induced changes in brain morphology occurred rapidly (range 66–94 and 26–79 min in METH-23°C and METH-29°C, respectively) and were independent of *time of METH exposure*. Despite much greater damage in METH-29°C than in METH-23°C, the mean time of exposure was shorter (58.13±5.82 vs. 81.88±3.96 min). No correlation with exposure time was found in each of the two groups analyzed separately (r=0.16 for 23°C and r=0.06 for 29°C) or as a whole (r=0.14).

4.5. Ultrastructural changes following METH administration—Rapid cellular changes seen at light microscopy following METH administration were further confirmed at the ultrastructural level using TEM (Figs. 9 and 10). At this level, several neuronal profiles located in the cortex were examined with special emphasis on the neuronal nucleolus and karyoplasm (Fig. 9, upper raw). As can be seen, a perfectly smooth rounded nuclear membrane containing a centralized nucleolus (arrow) was typical of normal brain tissue (a). The surrounding cytoplasm normally does not contain any vacuoles and the adjacent neuropil is quite compact. In contrast, degeneration of the nucleolus that became slightly excentric was seen in METH-23°C rats (c). Moreover, the nuclear membrane shows many foldings and vacuolation in the neuronal cytoplasm (*). Perinuclear membranes also often show degenerative changes (c). These nuclear changes were more profound in animals that received METH at 29°C (e). The nucleolus reached to one end of the karyoplasm and the nuclear envelope showed many irregular foldings (e). Cytoplasmic vacuolation (*) and degeneration of Nissl substance are clearly seen in this group of animals.

Degeneration of myelin and axons found using light microscopy with MBP staining in METH-treated animals was further confirmed at the ultratstructural level (see Fig. 9 bottom raw). The most marked changes in myelin vesiculation were seen in rats treated with METH at 29°C compared to those that received this drug at 23°C (d, f). Unlike control animals (b), METH-treated rats showed clear signs of damage to myelinated axons (arrows in b, d). Vesiculation of myelin (arrows) and axonal damage (*) are clearly evident in METH-treated rats at 23°C and are more pronounced in animals that received METH at 29°C (f). Thus, degeneration of myelinated axons, vesiculation of myelin (f, arrows), and edematous swelling of axonal membranes (f*) were quite frequent in this group. Normal animals exhibit a compact neuropil (b) and a non-vesiculated myelin sheath around the axons (arrow heads, a).

Since leakage of EB and albumin immunostaining showed a compromised barrier in animals treated with METH, the endothelial and surrounding neuropil were examined at the ultrastructural level in the cortex and hippocampus (Fig. 10). The cerebral capillary from the normal rat showed a compact neuropil and perivascular structures, endothelial cell surfaces

of the lumen were very smooth, and tight junctions (arrow) were clearly distinct (a and b). METH treatment markedly altered the endothelial cell surface in the lumen (c, d) and thus many endothelial cell bleb formations can be seen (arrow-head, d). The perivascular edema (*) and membrane vacuolation in the neuropil was apparent. These perivascular changes and endothelial cell membrane reactions were much more prominent in animals that received METH at 29°C (e, f, arrow heads). In these rats, swollen perivascular glial cells (*) and degeneration of pericapillary neuropil (e, f) was clearly visible. The endothelial cell membrane showed prominent bleb formation in this group and the endothelial cell cytoplasm was more electron dense (e, f) than the normal endothelium (a, b). Degeneration of perivascular glial cells was also more prominent in this group compared to rats treated with METH at 23°C (d, f). However, the tight junctions appeared to be intact in both METH-treated groups.

V. Conclusions

While slowly developing, selective, and irreversible damage of specific central neurons is a traditional focus of neurotoxic studies of METH, this work demonstrates that robust morphological abnormalities of neural and non-neural brain cells (i.e., glia, vascular endothelium, epithelium) occur rapidly (within 30–80 min) in various brain structures during acute METH intoxication. These abnormalities manifest as the distortion of neurons, overexpression of glial cells, vesiculation of myelin, and alterations in vascular endothelium and epithelium of the choroid plexus. While having some structural specificity, these acute morphological abnormalities appear to be widespread, tightly correlating with drug-induced brain and body hyperthermia and alterations in several basic homeostatic brain parameters including permeability of the BBB, tissue water and ion contents.

1. Mechanisms underlying METH-induced morphological brain abnormalities

Our study revealed that acute morphological alterations of brain cells during METH intoxication are tightly related to drug-induced increases in brain and muscle temperatures. The tight link between hyperthermia and structural brain damage was evident for the different brain structures and for both neuronal (Nissl staining), glial (GFAP immunoreactivity), endothelial (TEM), and epithelial (Nissl staining) cells. Although METH was used in all animals at the same dose, the counts of damaged neurons and abnormal GFAP-positive glial cells were drastically larger at 29°C than 23°C, correlating with stronger brain and body hyperthermia. Linear relationships between these parameters and brain temperature were also evident in individual animals, which showed greater morphological abnormalities at higher temperatures, irrespective of the ambient temperature during drug administration.

Since brain cells of various subtypes are exceptionally sensitive to high temperature (Bechtold and Brown, 2003; Chen et al., 2003; Oifa and Kleshchenov, 1985; Lee et al., 2000; Lin et al., 1991; Lin, 1997; Sharma and Hoopes, 2003), hyperthermia could be viewed as an important contributor to morphological abnormalities induced by METH. However, this does not mean that high temperature *per se* is the cause of these changes. Brain hyperthermia is not only a physical factor that could harm cells; it is also an integral physiological index of METH-induced metabolic activation (see Kiyatkin, 2005 for review) that also manifests as an enhanced release of multiple neuroactive substances, lipid peroxidation, and the generation of free radicals—numerous changes combined as oxidative stress (Seiden and Sabol, 1996; Cadet et al., 2007) as well as behavioral and autonomic activation. Although all these factors may contribute to structural brain abnormalities, it is quite difficult to separate them from each other because they are interdependent, representing different manifestations of METH-induced metabolic activation.

METH intoxication also results in a robust increase in BBB permeability, intra-brain water accumulation (edema), and serious alterations in brain ionic homeostasis. These changes, moreover, were tightly related to both the degree of hyperthermia and the intensity of structural brain damage. Therefore, breakdown of the BBB that allows the diffusion of endogenous albumin, water, several ions, and other neuroactive and potentially neurotoxic substances is another important contributor to brain pathology and the primary mechanism underlying decompensation of vital functions and lethality. While different chemical factors activated by METH could be involved in increased BBB permeability and edema formation, brain hyperthermia appears to play a crucial role since both these parameters strongly correlated with brain temperature. Such a role for hyperthermia in the leakage of the BBB and edema has been first suggested for environmental warming (Sharma et al., 1992; Cervos-Navarro et al., 1998); the intensity of these changes was strongly dependent upon the strength of body hyperthermia as evaluated by rectal temperature measurements.

2. Common features and structural selectivity of METH-induced cellular alterations

To define the common features and structural specificity of METH-induced morphological and functional perturbations, our examinations were conducted in four brain structures – the cortex, hippocampus, thalamus, and hypothalamus. As shown above, these structures had some differences in tested parameters in normal conditions as well as some degree of specificity following METH impact. Despite evident between-structure differences in tissue water content in control brains, the increase was relatively similar in different brain structures at 23°C (~1.3%; see Fig. 5) and dramatically amplified at 29°C (~2.6–3.1%), suggesting severe edema within the brain as a whole. Robust water accumulation in brain tissue was associated with a clearly pathological brain hyperthermia (>41°C), strong increases in Na^+, K^+, Cl^- in all brain structures, and maximal increases in albumin- (×22–75) and GFAP-positive (×8–13) cells. These animals also showed especially strong brain cell abnormalities that were evident in each structure and with each morphological and histochemical test. Degeneration of cellular elements in the nucleus, condensed cytoplasm, and irregular folding of the nuclear membrane found with electron microscopy denotes clear cell damage, which would possibly lead to cellular disintegration. The extreme character of these changes is related to the fact that if our experiment is not terminated and brains not taken for examinations, some of these animals (especially in the METH-29°C group) will naturally die within the next 10–30 min. Therefore, these changes appear to reflect acute pathological brain perturbations that could result in profound functional disturbances and lethality. While edema and ionic misbalance appears to be widespread within the brain, individual brain structures differed in the extent of morphological abnormalities. The numbers of damaged neuronal and glial cells were both greater in the cortex and hippocampus but smaller in the thalamus and hypothalamus. While the reasons of this structural specificity to damage remains unknown, the cortex and hippocampus also showed much stronger increases in EB penetration and albumin immunostaining than the thalamus and hypothalamus, suggesting a tight link between BBB leakage and structural damage. Although brain damage was evident in each cellular subtype (neurons, glial cells, vascular endothelium, axons), especially profound abnormalities were found in epithelial cells of the choroid plexus—a critical substrate of the blood-cerebrospinal fluid (CSF) barrier (Keep et al., 2005). Because of the role of this organ in the production of the CSF, the damage of epithelial cells and destruction of gap junctions could strengthen edema and ionic disbalance, thus amplifying cellular damage in other brain structures. While it is unclear why this structure is so sensitive to damage during METH intoxication, it has an exceptionally high blood flow (Faraci et al., 1988) and mitochondrial density (Keep and Jones, 1990) compared to other structures, supporting a presumed link between metabolic activity and cellular damage following thermal impact (see Kiyatkin, 2005 for review).

3. Reversibility/Irreversibility of structural alterations

Although our data indicate that acute METH intoxication results in rapidly developing morphological abnormalities in neural and non-neural brain cells, it remains unclear whether these abnormalities are reversible or irreversible in nature. Dramatic changes in cellular elements (e.g., degeneration of some neuronal nucleus, endothelial cell membrane bleb-formation, vesiculation of myelin and vacuolation in the neuropil with clear signs of synaptic damage and swelling), especially evident in the METH-29°C group, appear to be inconsistent with normal cell functions, pointing at irreversible damage. However, some of these changes appear to be transient and reversible and they could dissiapate after basic homeostatic parameters are restored to baseline. In contrast to the unusually large numbers of GFAP-positive glial cells found in this study during acute METH intoxication (×3–7 and ×7–12 vs. control in 23 and 29°C groups, respectively), much weaker increases in GFAP-positive cells were found in rats in days after acute METH impact (Miller and O'Callaghan, 1994; O'Callaghan and Miller, 1994). These changes, moreover, appeared at 12–24 hrs, peaked at the second day, and remained elevated for seven days after a single METH exposure. In contrast to the widespread alterations in our study, these changes were evident only in the striatum and to a lesser degree in the cortex, correlating with decreased dopamine levels in these structures. While in light of the profound morphological abnormalities found during acute METH intoxication we can speculate that they could result in irreversible cellular damage, this issue needs to be examined further. While rapid and strong increases in GFAP immunostaining have been reported previously during environmental warming (~2–3 hours; Sharma et al., 1992; Cervos-Navarro et al., 1998) and following acute traumatic injury to the brain and spinal cord (30–40 min; Cervos-Navarro et al., 1998; Gordth et al., 2006), different mechanisms appear to mediate rapid and slow glial reactions. GFAP expression is usually thought of as a late outcome of traumatic, ischemic, or hypoxic insults or a correlate of various neurodegenerative diseases (Finch, 2003; Hausmann, 2003; Gordth et al., 2006), representing astrogliosis (Norton et al., 1992; O' Callaghan, 1993). In contrast, rapid GFAP expression seen in association with strong edema (environmental warming, acute trauma, METH intoxication) could reflect the interaction of antibodies with GFAP somehow released or made available during membrane damage. Thus, binding sites to GFAP could be increased due to acute breakdown of the BBB and associated edema rather than proliferation of astrocytes or elevated levels of GFAP proteins that require more time. Since damage of astrocytes and swelling of the astrocytic end foot results in increased binding of GFAP antibodies (Bekay et al., 1977; Bondarenko and Chesler, 2001; Gordth et al., 2006), this reaction could reflect acute, possibly reversible, damage of glial cells. Relatively smaller numbers of damaged neural cells in the post-intoxication period compared to acute METH intoxication (see Bowyer and Ali, 2006) could also be related to their rapid scavenging, making it difficult to detect them using traditional techniques. Although the issue of the extent of damage and its reversibility remains unanswered and requires additional studies, it is likely that rapid cell abnormalities may initiate cascades that could precipitate cellular and molecular dysfunctions, leading to neurodegeneration—the most dangerous outcome of chronic abuse with amphetamine-like drugs.

Acknowledgments

This research was supported by the Intramural Research Program of the NIH, NIDA.

References

Alberts DS, Sonsalla PK. Methamphetamine-induced hyperthermia and dopaminergic neurotoxicity in mice: pharmacological profile of protective and nonprotective agents. J. Pharmacol. Exp. Ther. 1995; 275:1104–1114. [PubMed: 8531070]

Ali SF, Newport GD, Holson RR, Slikker W, Bowyer JF. Low environmental temperatures or pharmacological agents that produce hypothermia decrease methamphetamine neurotoxicity in mice. Brain Res. 1994; 658:33–38. [PubMed: 7530580]

Bechtold DA, Brown IR. Induction of Hsp27 and Hsp32 stress proteins and vimentin in glial cells of the rat hippocampus following hyperthermia. Neurochem. Res. 2003; 28:1163–1173. [PubMed: 12834255]

Bekay L, Lee JC, Lee GC, Peng GR. Experimental cerebral concussion: An electron microscopic study. J. Neurosur. 1977; 47:525–531.

Blezer, E. Techniques for measuring the blood-brain barrier integrity. In: de Vries, E.; Prat, A., editors. The Blood-Brain Barrier and Its Microenvironment. New York: Taylor & Francis; 2005. p. 441-456.

Bondarenko A, Chesler M. Rapid astrocyte death induced by transient hypoxia, acidosis, and extracellular ion shifts. Glia. 2001; 34:134–142. [PubMed: 11307162]

Bowyer JF, Gough B, Slikker W, Lipe GW, Wewport GD, Holson RR. Effects of a cold environment or age on methamphetamine-induced dopamine release in the caudate putamen of female rats. Pharmacol. Biochem. Behav. 1993; 44:87–98. [PubMed: 8094252]

Bowyer JF, Ali S. High doses of methamphetamine that cause disruption of the blood-brain barrier in limbic areas produce extensive neuronal degeneration in mouse hippocampus. Synapse. 2006; 60:521–532. [PubMed: 16952162]

Brown PL, Wise RA, Kiyatkin EA. Brain hyperthermia is induced by methamphetamine and exacerbated by social interaction. J. Neurosci. 2003; 23:3924–3929. [PubMed: 12736362]

Brown PL, Kiyatkin EA. Brain hyperthermia induced by MDMA (“ecstasy”): modulation by environmental conditions. Eur. J. Neurosci. 2004; 20:51–58. [PubMed: 15245478]

Brown PL, Kiyatkin EA. Fata intra-brain heat accumulation induced by methamphetamine at normothermic conditions in rats. Int. J. Neurodegen. Neuroregen. 2005; 1:86–90.

Cadet JL, Krasnova IN, Jayanthi S, Lyles J. Neurotoxicity of substituted amphetamines: molecular and cellular mechanisms. Neurotox. Res. 2007; 11:183–202. [PubMed: 17449459]

Cervos-Navarro J, Sharma HS, Westman J, Bongcum-Rudloff E. Glial cell reactions in the central nervous system following heat stress. Progr. Brain Res. 1998; 115:241–274.

Chen YZ, Xu RX, Huang QJ, Xu ZJ, Jiang XD, Cai YO. Effect of hyperthermia on tight junctions between endothelial cells of the blood-brain barrier model in vitro. Di Yi Jun Da Xue Xue Bao. 2003; 23:21–24.

Devis WM, Hatoum HT, Walters IW. Toxicity of MDA (2.4-methylenedioxyamphetamine) considered for relevance to hazards of MD<A (Ecstasy) abuse. Alcohol Drug Res. 1987; 7:123–134. [PubMed: 2881551]

De Vito MJ, Wagner GC. Methamphetamine-induced neuronal damage: a possible role for free radicals. Neuropharmacology. 1989; 28:1145–1150. [PubMed: 2554183]

Doepp F, Schreiber SJ, Munster T, Rademacher J, Klingbiel R, Valdueza JM. How does the bloods leave the brain? A systematic untrasound analysis of central venous drainage pattern. Neuroradiol. 2004; 46:565–570.

Ehrlich, P. Gesammelte Arbeiten zur Immunitatsforschung. Berlin: 1904. Uber die Beziehung chemischer onstitution, Verteilung, und pharmacologischer Wirkung.

Esposito P, Cheorghe D, Kendere K, Pang X, Connoly R, Jaconson S, Theodorides TC. Acute stress increases permeability of the blood-brain barrier through activation of brain must cells. Brain Res. 2001; 888:117–127. [PubMed: 11146058]

Estler CJ. Dependence on age of metamphetamine-produced changes in thermoregulation and metabolism. Experientia. 1975; 31:1436–1437. [PubMed: 1213067]

Faraci FM, Mayham WG, Williams JK, Heistad DD. Effects of vasoactive stimuli on blood flow to choroid plexus. Am. J. Physiol. 1988; 254:H286–H291. [PubMed: 3344819]

Finch CE. Neurons, glia, and plasticity in normal brain aging. Neurobiol. Aging. 2003; 24 Suppl 1:S123–S127. [PubMed: 12829120]

Farfel GM, Seiden LS. Role of hyperthermia in the mechanism of protection against serotoninergic toxicity. II. Experiments with methamphetamine, p-chloroamphetamine, fenfluramine, dizocilpine and dextromethorphan. J. Pharmacol. Exp. Ther. 1995; 272:868–875. [PubMed: 7853205]

Gordh T, Chu H, Sharma HS. Spinal nerve lesion alters blood-spinal cord barrier function and activates astrocytes in the rat. Pain. 2006; 124:211–221. [PubMed: 16806707]

Hausmann ON. Post-traumatic inflammation following spinal cord injury. Spinal Cord. 2003; 41:369–378. [PubMed: 12815368]

Iwagami Y. Changes in the ultrastructure of human cell related to certain biological responses under hyperthermic culture conditions. Human Cell. 1996; 9:353–366. [PubMed: 9183669]

Kalant H. The pharmacology and toxicology of “ecstasy” (MDMA) and related drugs. Can. Med. Ass. J. 2001; 165:917–928. [PubMed: 11599334]

Kalant H, Kalant OJ. Death in amphetamine users: causes and rates. Can. Med. Assoc. J. 1975; 112:299–304. [PubMed: 1089034]

Keep RF, Jones HC. A morphometric study on the development of the lateral choroids plexus, choroids plexus capillaries and ventricular ependyma in the rat. Dev. Brain Res. 1990; 56:47–53. [PubMed: 2279331]

Keep, RF.; Ennis, SR.; Xiang, J. The blood-CSF barrier and cerebral ischemia. In: Zheng, W.; Chodobski, A., editors. The blood-cerebrospinal fluid barrier. Boca Raton: CRC Press; 2005. p. 345-360.

Kiyatkin EA, Brown PL. Modulation of physiological brain hyperthermia by environmental temperature and impaired blood outflow in rats. Physiol. Behav. 2004; 83:467–474. [PubMed: 15581669]

Kiyatkin EA. Brain hyperthermia as physiological and pathological phenomena. Brain Res. Rev. 2005; 50:27–56. [PubMed: 15890410]

Kiyatkin EA. Drug-induced brain hyperthermia: Mechanisms and functional implications. Int. J. Neurodegen. Neuroregen. 2006; 2:168–174.

Kiyatkin EA, Brown PL, Sharma HS. Brain edema and breakdown of blood-brain barrier during methamphetamine intoxication: Critical role of brain temperature. Eur. J Neurosci. 2007; 26:1242–1253. [PubMed: 17767502]

Lee SY, Lee SH, Akuta K, Uda M, Song CW. Acute histological effects of interstitial hyperthermia on normal rat brain. Int. J. Hyperthermia. 2000; 16:73–83. [PubMed: 10669318]

Lepock JR. Cellular effects of hyperthermia: relevance to the minimum dose for thermal damage. Int. J. Hyperthermia. 2003; 19:252–266. [PubMed: 12745971]

Lin PS, Quamo S, Ho KC, Gladding J. Hyperthermia enhances the cytotoxic effects of reactive oxygen species to Chinese hamster cells and bovine endothelial cells *in vitro*. Radiat. Res. 1991; 126:43–51. [PubMed: 1850533]

Lin M-T. Heatstroke-induced cerebral ischemia and neuronal damage. Involvement of cytokines and monoamines. Ann. N.Y. Acad. Sci. 1997; 813:572–580. [PubMed: 9100936]

Miller DB, O’Callaghan JP. Environment-, drug- and stress-induced alterations in body temperature affect the neurotoxicity of substituted amphetamines in the C57BL/6J mouse. J. Pharmacol. Exp. Ther. 1994; 270:752–760. [PubMed: 8071868]

Miller DB, O’Callaghan JP. Elevated environmental temperature and methamphetamine neurotoxicity. Environ. Res. 2003; 92:48–53. [PubMed: 12706754]

Makisumi T, Yoshida K, Watanabe T, Tan N, Murakami N, Morimoto A. Sympath-adrenal involvement in methamphetamine-induced hyperthermia through skeletal muscle hypermethanolism. Eur. J. Pharmacol. 1998; 363:107–112. [PubMed: 9881575]

Norton WT, Aquino DA, Hozumi I, Chiu F-C, Brosnan CF. Quantitative aspects of reactive gliolis: A review. Neurochem. Res. 1992; 17:877–885. [PubMed: 1407275]

O’Callaghan JP. Quantitative features of reactive gliolis following toxicant-induced damage of the CNS. Ann. N.Y. Acad. Sci. 1993; 679:195–210. [PubMed: 8512183]

O’Callaghan JP, Miller DB. Neurotoxicity profiles of substituted amphetamines in the C57BL/6J mouse. J. Pharmacol. Exp. Ther. 1994; 270:741–751. [PubMed: 8071867]

Oifa AI, Kleshchnov VN. Ultrastructural analysis of the phenomenon of acute neuronal swelling. Zh. Nevropatol. Psikhiatr. Im S.S. Korsakova. 1985; 85:1016–1020. [PubMed: 4041105]

Ovadia H, Abramsky O, Feldman S, Weidenfeld J. Evaluation of the effects of stress on the blood-brain barrier: critical role of the brain perfusion time. Brain Res. 2001; 905:21–25. [PubMed: 11423075]

Papoport, SI. Blood-brain barrier in physiology and medicine. New York: Raven Press; 1976.

Ricaurte GA, Schuster CR, Seiden LS. Long-term effects of repeated methamphetamine administration on dopamine and serotonin neurons in the rat brain: a regional study. Brain Res. 1980; 193:153–163. [PubMed: 7378814]

Riddle EL, Fleckenstein AE, Hanson GR. Mechanisms of methamphetamine-induced dopaminergic neurotoxicity. The AAPS Journal. 2006; 8(2) Article 48 http://www.aapsj.org.

Romanovsky AA, Ivanov AI, Shimansky YP. Ambient temperature for experiments in rats: a new method for determining the zone of thermal neutrality. J. Appl. Physiol. 2002; 92:2667–2679. [PubMed: 12015388]

Sandoval V, Hanson GR, Fleckenstein AE. Methamphetamine decreases mouse striatal dopamine transport activity: roles of hyperthermia and dopamine. Eur. J. Pharmacol. 2000; 409:265–271. [PubMed: 11108820]

Seiden LS, Sabol KE. Methamphetamine and methylenedioxymethamphetamine neurotoxicity: possible mechanisms of cell destruction. NIDA Res. Monogr. 1996; 163:251–276. [PubMed: 8809863]

Sharma HS. Pathophysiology of blood-spinal cord barrier in traumatic injury and repair. Curr. Pharm. Des. 2005; 11:1353–1389. [PubMed: 15853669]

Sharma HS. Methods to produce hyperthermia-induced brain dysfunction. Prog. Brain Res. 2007; 162:173–199. [PubMed: 17645920]

Sharma HS, Ali SF. Alterations in blood-brain barrier function by morphine and amphetamine. Ann. N.Y. Acad. Sci. 2006; 1074:198–224. [PubMed: 17105918]

Sharma HS, Dey PK. Influence of long-term immobilization stress on regional blood-brain permeability, cerebral blood flow and 5-HT levels in conscious normotensive young rats. J. Neurol. Sci. 1986; 72:61–76. [PubMed: 2936871]

Sharma HS, Hoopes PJ. Hyperthermia-induced pathophysiology of the central nervous system. Int. J. Hyperthermia. 2003; 19:325–354. [PubMed: 12745974]

Sharma HS, Kiyatkin EA. Rapid morphological brain abnormalities during acute methamphetamine intoxication in the rat: An experimental study using light and electron microscopy. J. Chem. Neuroanat. 2009; 37:18–32. [PubMed: 18773954]

Sharma HS, Zimmer C, Westman J, Cervos-Navarro J. Acute systemic heat stress increases glial fibrillary acidic protein immunoreactivity in brain. An experimental study in the conscious normotensive young rats. Neuroscience. 1992; 48:889–901. [PubMed: 1630627]

Stephans SE, Yamamoto BK. Methamphetamine-induced neurotoxicity: role for glutamate and dopamine influx. Synapse. 1994; 17:203–209. [PubMed: 7974204]

Watson P, Shirreffs SM, Maughan RJ. Blood-brain barrier integrity may be threatened by exercise in a warm environment. Am. J. Physiol. 2005; 288:R1689–R1694.

Willis WT, Jackman MR, Bizeau ME, Pagliassotti MJ, Hazel JR. Hyperthermia impairs liver mitochondrial functions. Am. J. Physiol. 2000; 278:R1240–R1246.

Woolverton WL, Ricaurte GA, Forno L, Seiden LS. Long-term effects of chronic methamphetamine administration in rhesus monkeys. Brain Res. 1989; 486:73–78. [PubMed: 2720435]

Yamamoto BK, Zhu W. The effect of methamphetamine on the production of free radicals and oxidative stress. J. Pharmacol. Exp. Ther. 1998; 287:107–114. [PubMed: 9765328]

Yamamoto H. The central effects of xylopinine in mice. Jap. J. Pharmacol. 1963; 13:230–239. [PubMed: 14097554]

Zlokovic BV. The blood-brain barrier in health and chronic neurodegenerative disorders. Neuron. 2008; 57:178–201. [PubMed: 18215617]

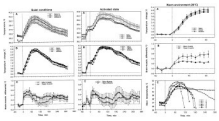

Fig. 1.

Effects of methamphetamine (9 mg/kg, sc) on brain (NAcc and hippocampus) and muscle temperatures in rats in three conditions (left, quiet rest at 23°C; middle, social interaction with female at 23°C; right, quiet rest at 29°C). Graphs represent absolute and relative temperature changes as well as brain-muscle differentials. Filled symbols mark values significantly different from baseline.

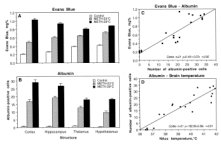

Fig. 2.

Mean (±sem) values of Evans Blue concentrations (A) and numbers of albumin-positive cells (B) in individual brain structures after saline (control) and methamphetamine administration at 23°C and 29°C. C shows correlative relationships between concentrations of Evans Blue and numbers of albumin-positive cells in the cortex. D shows correlative relationships between the numbers of albumin-positive cells in the cortex and NAcc temperatures. Each graph shows regression equation, regression line, and correlation coefficient (r).

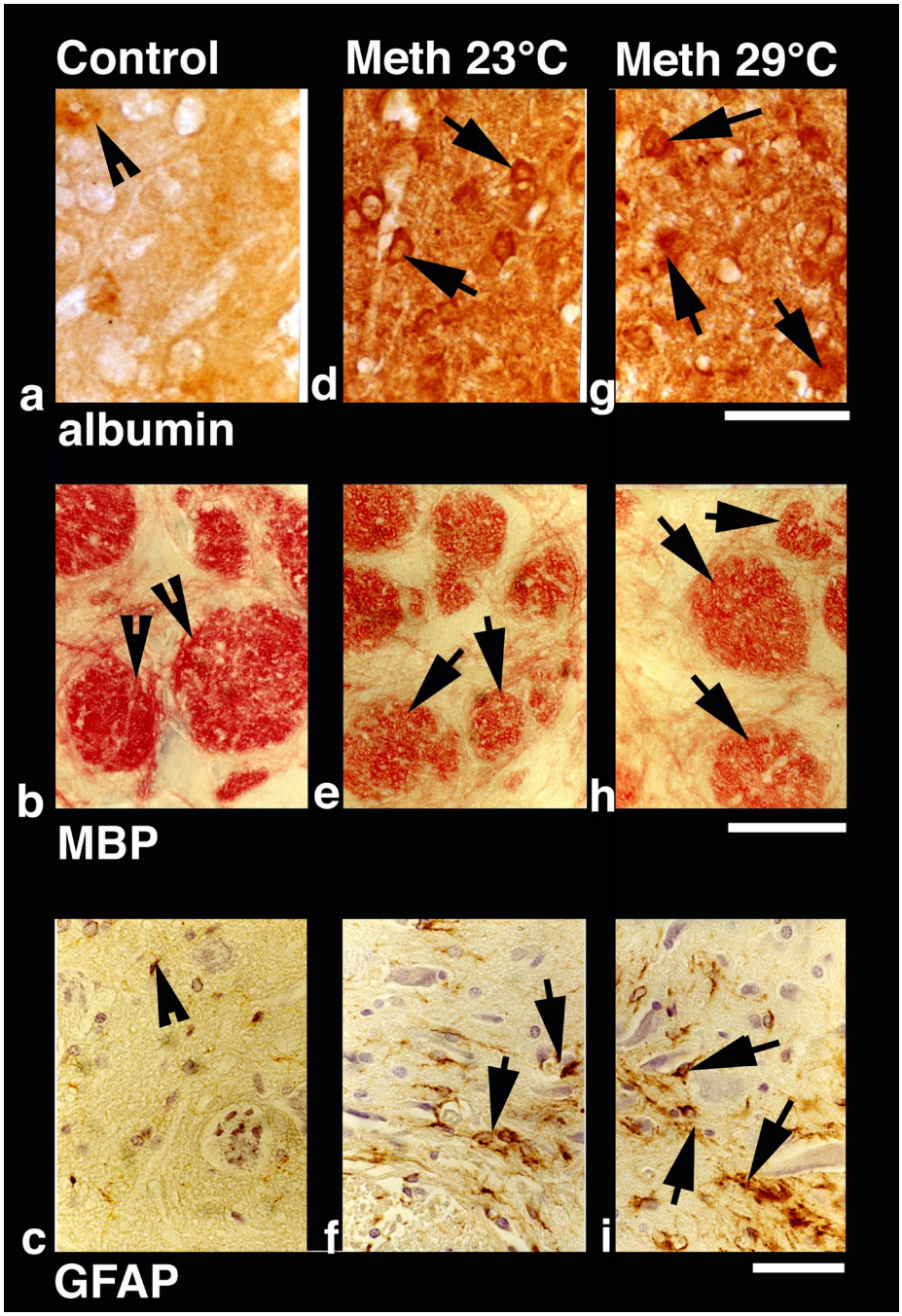

Fig. 3.

Immunohistochemical changes in albumin (a, d, g), myelin basic protein (MBP; b, e, g) and glial fibrillary acidic protein (GFAP; c, f, i) in control (left vertical panel) and METH-treated rats (23°: middle vertical panel and 29°C: right vertical panel). Compared to weak albumin immunoreactivity in control (a, arrowhead), METH-treated rats had stronger immonoreactivity (arrows in d and g). Expansion of neuropil and sponginess is also evident in the surrounding background. Bar (a, d, g) = 40 μm. In contrast to intense red myelin bundles and dense red fibers in control (b, arrowheads, b), diminution of red staining in the bundles and fibers (e, arrows) was seen in METH-treated rats (e). This degradation of MBP was most prominent in the rats treated with METH at 29° C (arrows, h). Bar (b, e, h) = 30

μm. GFAP immunostaining was prominent in METH-treated rat at 29° C (i, arrows) compared to 23°C (f, arrows). Control rats (c) occasionally show few GFAP positive astrocytes (arrowhead). Reactive astrocytes were located around the nerve cells and microvessels, and distributed in wide regions in the neuropil. Damaged neurons can also be seen in the background. Bar (c, f, i) = 40 μm.

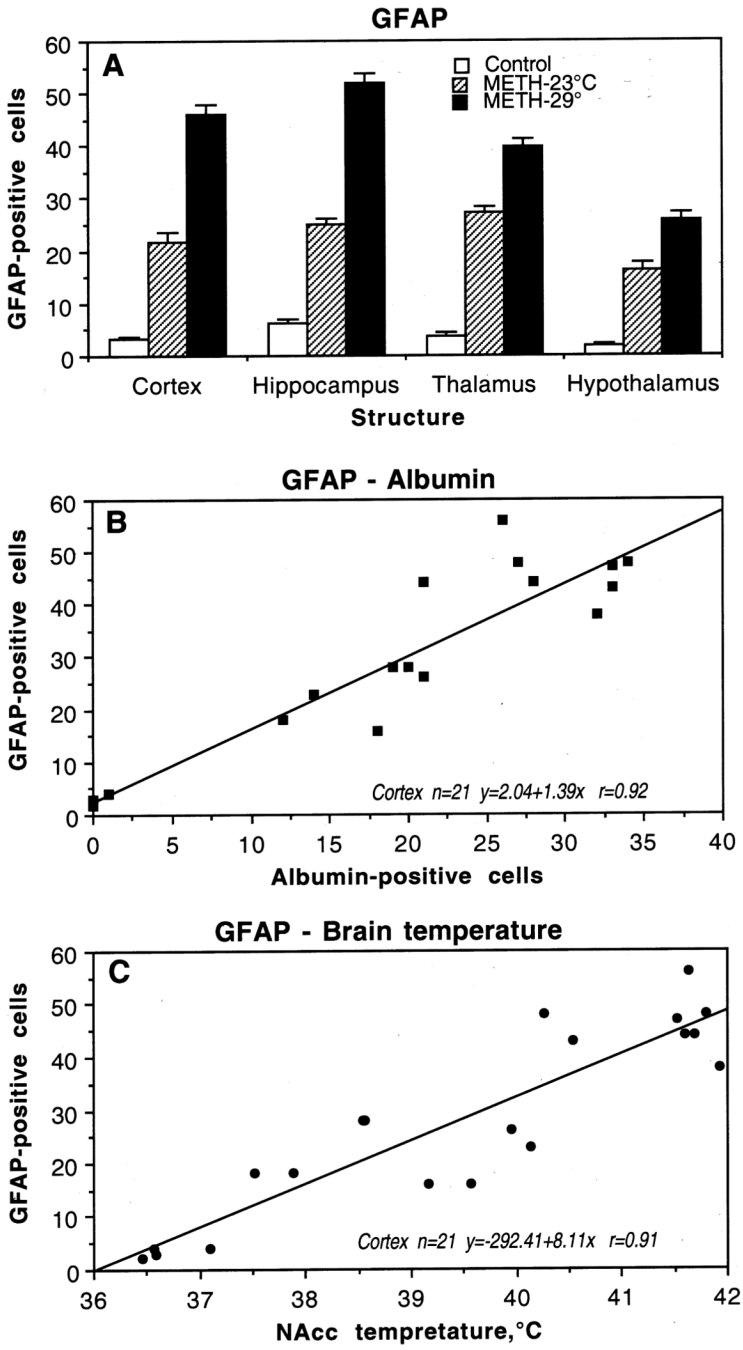

Fig. 4.

Mean (±sem) numbers of GFAP-positive cells in individual brain structures of rat brains taken after saline (control) and methamphetamine administration at 23°C and 29°C (A). B shows correlative relationships between the numbers of albumin- and GFAP-positive cells in the cortex. C shows correlative relationships between the numbers of GFAP-positive cells in the cortex and NAcc temperatures. Each graph shows regression equation, regression line, and correlation coefficient (r).

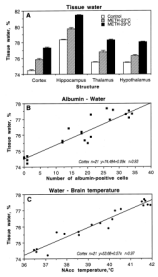

Fig. 5.

Mean (±sem) concentrations of tissue water in individual brain structures after saline (control) and methamphetamine administration at 23°C and 29°C (A). B shows correlative relationships between the numbers of albumin-positive cells and water in the cortex. C shows correlative relationships between tissue water in the cortex and NAcc temperatures. Each graph shows regression equation, regression line, and correlation coefficient (r).

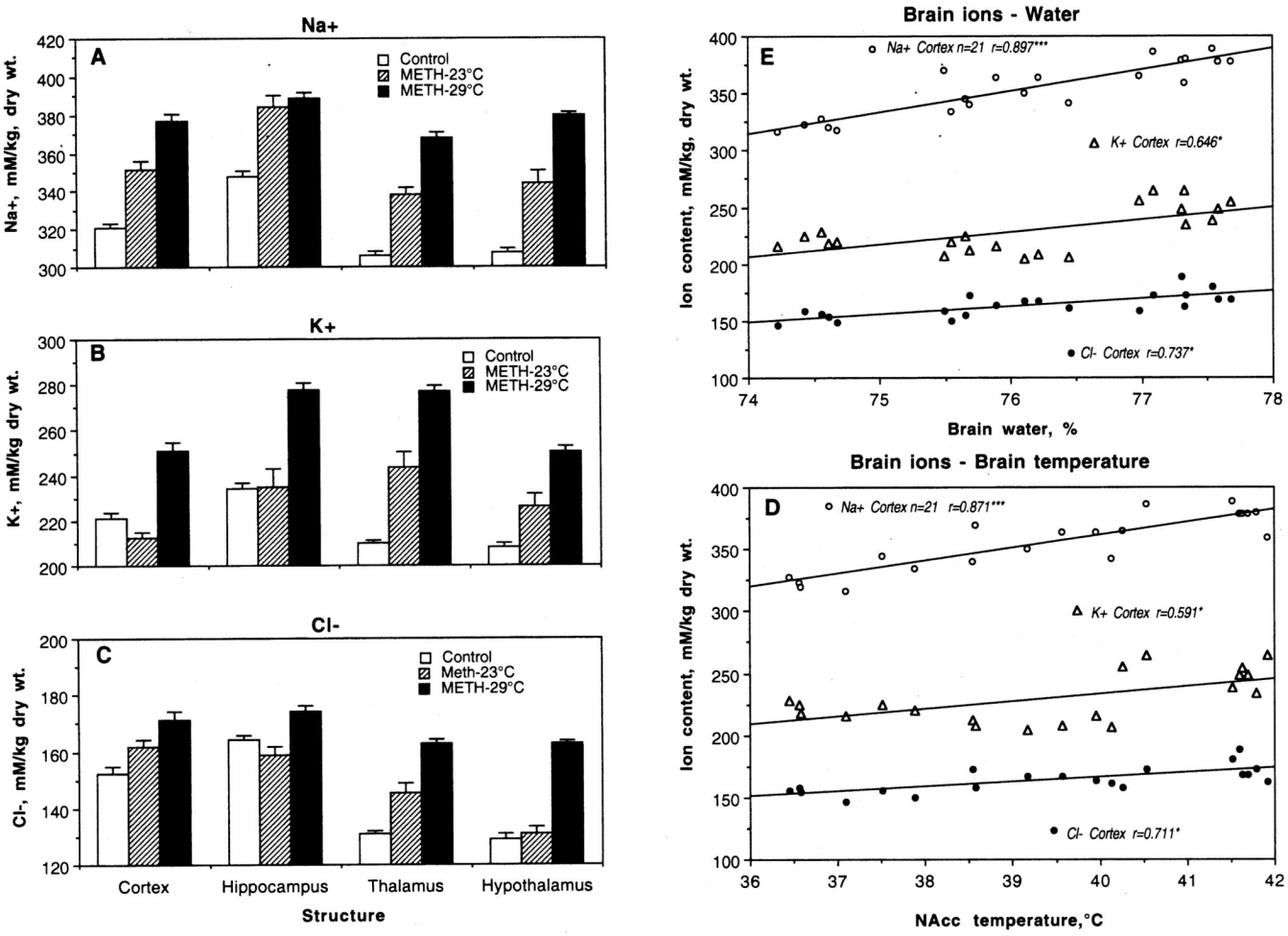

Fig. 6.

Mean (±sem) concentrations of Na^+ (A), K^+ (B) and Cl^- (C) in individual brain structures of rat brains taken after saline (control) and methamphetamine administration at 23°C and 29°C (A). E shows correlative relationships between ion content and tissue water in the cortex. D shows correlative relationships between ion content in the cortex and NAcc temperatures. Each graph shows regression line and correlation coefficient (r).

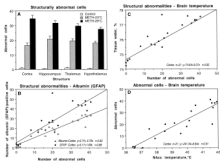

Fig. 7.

Mean (±sem) numbers of structurally abnormal cells in individual brain structures after saline (control) and methamphetamine administration at 23°C and 29°C (A). B shows correlative relationships between structural abnormalities and numbers of albumin- and GFAP-positive cells in the cortex. C shows correlative relationships between the numbers of abnormal cells and tissue water. D shows correlative relationships between the numbers of abnormal cells in the cortex and NAcc temperatures. Each graph shows regression equation, regression line, and correlation coefficient (r).

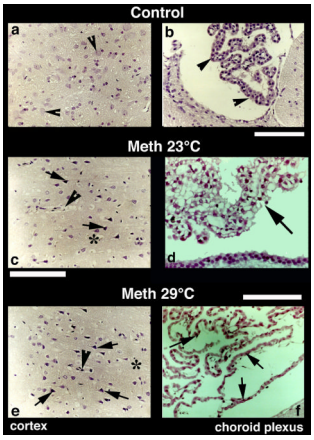

Fig. 8.

Nissl-stained sections from the cerebral cortex (left panel) and choroid plexus (right panel) from control (a, b), METH-23°C (c, d) and METH-29°C (e, f) treated rats. Most of the nerve cells in the control cortex are healthy with a distinct nucleus in the center. Only a few nerve cells show condense cytoplasm (arrowheads, a). On the other hand, dark and distorted neurons were frequent in METH-treated rats (c and e; arrows). Sponginess (*) and perivascular edema (arrowheads; c, e) are frequent in METH-treated rats; the changes are more pronounced at 29° C (e) compared to 23° C (c). Bars (a, c, e) = 50 μm. Nissl-stained choroid epithelial cells in control (b) show compact and densely packer epithelial cells with distinct cell nucleus (arrow, b). METH treatment at 23° C resulted in mild degeneration of choroid epithelium (arrows, d). The epithelial cell nucleus also appears to be disintegrated (d). These degenerating changes in the choroidal epithelium is most pronounced in the rat that received METH at 29° C (arrows, f). Bars (b = 50 μm; d = 40 μm, f = 60 μm).

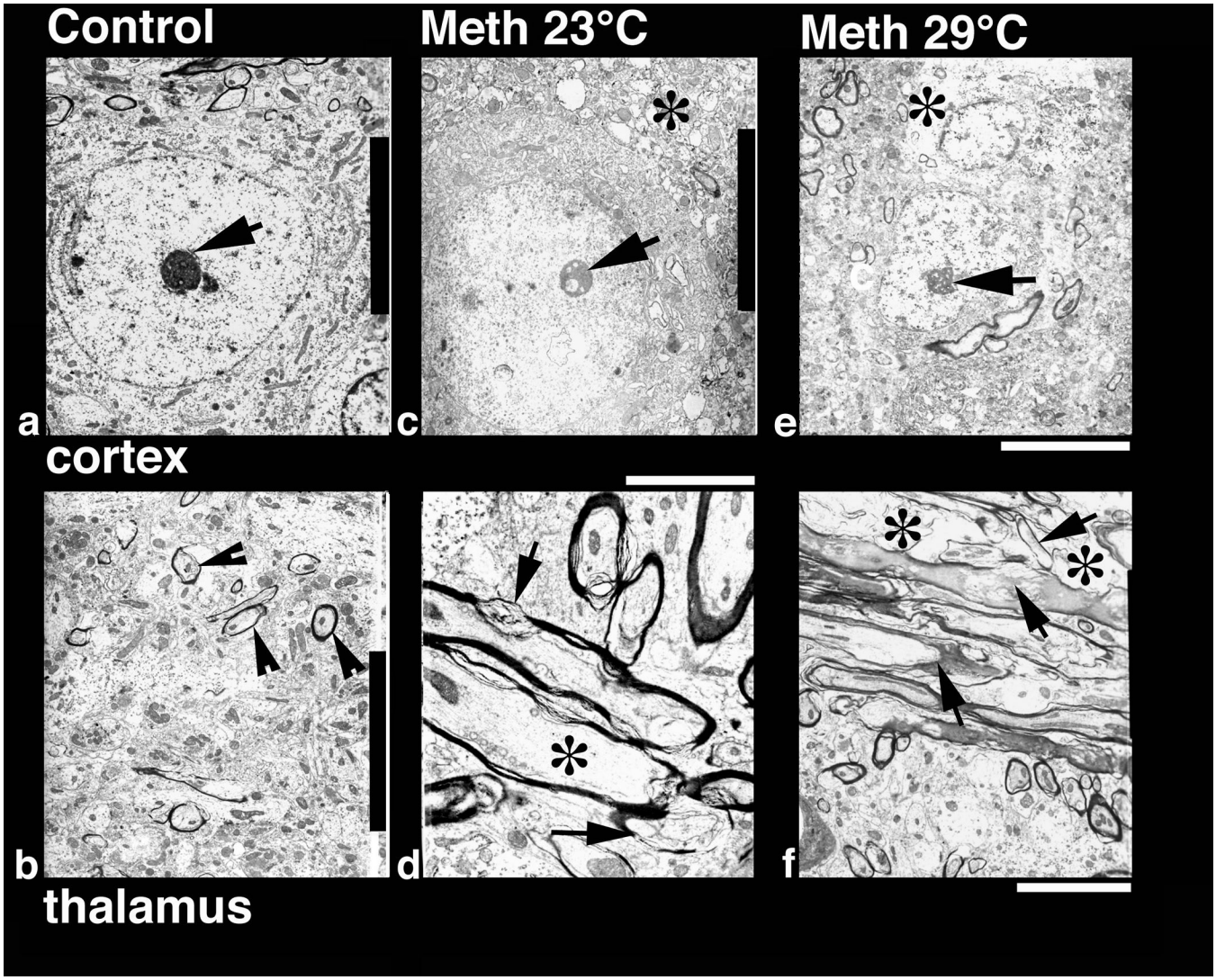

Fig. 9.

Low-power transmission electron micrograph from the cortex (upper panel) and thalamus (lower panel) showing neuronal nuclear (a, c, e) and axonal changes (b, d, f) in control (a, b), METH-23° C (c, d) and METH-29° C (e, f) groups. The neuronal nucleus in control rat shows a smooth nuclear envelop with dark granular karyoplasm containing a central nucleolus (a, arrow). The nerve cell cytoplasm is compact and condensed without any vacuoles. On the other hand, less electron-dense karyoplasm with an eccentric nucleolus showing degenerative changes is seen in the METH-23°C group (c, arrow). The nuclear membrane showed irregular foldings and vacuolation (*) in the neuropil including cytoplasm. These changes in the cell nucleus were much more aggravated in rat treated with METH at 29°C (e); degeneration of nuclear membrane and surrounding neurnal cytoplasm is clearly evident in this slice. The nucleolus is further degenerated (arrow) and became more eccentric (e). Bar: a–c = 1 μm. Axonal changes in the thalamus of METH-treated rats at 23°C (d) show profound myelin vesiculation (arrow) and edematous swelling (*, d). These changes were stronger in rats treated with METH at 29° C (f). In this group, the myelin vesiculation (arrows) and degeneration of axons were clearly evident (*, f). On the other hand, normal rat exhibited a compact neuropil with normal myelinated axons (arrow

heads, b). Signs of vacuolation and edema are largely absent in control group (a, b). Bars: b = 1500 nm, d = 800 nm; f = 600 nm.

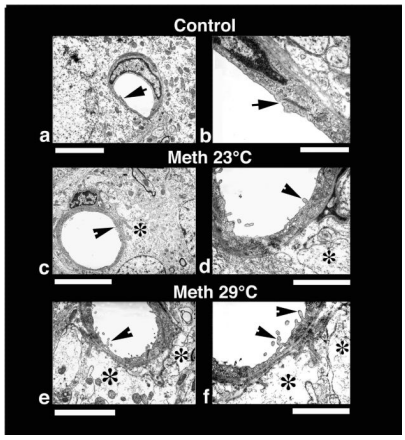

Fig. 10.

Low-power (left panel) and high-power (right panel) transmission electronmicrographs (left panel) showing a cerebral capillary and the surrounding neuropil in control (a and b) and METH-treated brain (c and d, 23°; e and f 29° C). Normal cerebral capillary has smooth luminal surface and a compact, dense neuropil surrounding it and normal tight junctions (a, arrow). The normal capillary also has distinct tight junctions (b, arrow) and the underlying glial cells (astrocyte) do not exhibit any apparent signs of perivascular edema (b). METH treatment at 23°C resulted in endothelial cell reaction and swelling of the perivascular astrocyte (*, c). The endothelial luminal surface exhibited few distinct bleb formations (arrow head) indicating the process of enhanced vesicular transport or alterations in membrane transport properties (d, for details see text). Swollen perivascular astrocytes and its processes (*) are evident in this METH-treated rat (d). These ultratstructural changes, e.g., bleb formation and perivascular edema, were much more aggravated in the rat after METH treatment at 29°C (e, f). Thus, spreading out of small membrane vesicles and elongated bleb formation could be seen in this group (arrow heads). Swelling of astrocytes (*) and disintegration of astrocytic cytoplasm indicating water filled cells are clearly visible (*, f). The endothelial cell cytoplasm in METH-treated rats shows much condense cytoplasm (d, f) compared to control (a, b). Bars: a, c = 1 μm, e = 2 μm; b = 500 nm; d = 800 nm; f = 600 nm.